GW investigation of interface-induced correlation effects on transport properties in realistic nanoscale structures

Changsheng Li, M. Bescond,* and M. Lannoo
IM2NP, UMR CNRS 6242, Bat. IRPHE, 13384 Marseille, France
(Received 3 August 2009; revised manuscript received 20 October 2009; published 19 November 2009)

We report a theoretical investigation of long-range correlation effects induced by the presence of interfaces in realistic semiconductor based nanoscale structures. This is performed within the so-called GW approximation of Hedin and Lundqvist in which we isolate the contribution of the interfaces with dielectrics or metallic electrodes to the exchange-correlation self-energy. We incorporate these correlation effects self-consistently into the solution of the Schrödinger equation and calculate its influence on transport properties in realistic nanoscale transistors. Numerical results show that the self-energy correction due to dielectric mismatch can be comparable to the direct quantum confinement effect. With the decrease in size, this correlation effect has a significant impact on the current-voltage characteristics and contributes to the increase in variability in ultimate nanoscale transistors.

DOI: 10.1103/PhysRevB.80.195318 PACS number(s): 73.63.−b, 71.45.Gm, 72.10.−d

I. INTRODUCTION

Recent progress in fabrication techniques has motivated the physicists community to consider quantum effects appearing in nanometer scale devices.[1,2] With the reduction in size, the effect of quantum confinement for semiconductors has been extensively studied.[3,4] On the other hand, the introduction of materials such as high-κ oxides (i.e., with a high dielectric constant) has also generated strongly inhomogeneous dielectric regions in MOS (metal-oxide-semiconductor) devices. Understanding the effects of the dielectric environment on the transport properties has then attracted recently a growing attention.[5,6] These inhomogeneities can modify the gate efficiency and create a self-energy correction whose magnitude is proportional to the dielectric constant ratio. Indeed in the nanometer range an electron added into the active region repels nearby electrons to the interfaces of the system, inducing a so-called image charge distribution. In this context, we theoretically study the influence of the image effects arising from interfaces polarization in realistic nanoscale structures. The interaction between the electron and its own image charge distribution at the interfaces is a long-range correlation effect, which is not included in the conventional calculations for out of equilibrium open systems. It should be described within a many-body framework such as the GW method of Hedin and Lundquist.[7]

Unfortunately, most calculations performed on nanoscale devices are based on the use of a Schrödinger-Poisson self-consistent procedure which is nothing else than the conventional Hartree approximation. However at small dimensions it is likely that interface-induced correlation effects will become important. A pioneering work in this direction is due to Inkson[8] who showed that image charge effects can drastically reduce the semiconductor gap in the neighborhood of a metal-semiconductor interface. Such effects cannot be predicted by local density approximation (LDA) calculations but it was shown in Ref. 9 that they are naturally included in the so-called GW approximation. In fact, as shown in Ref. 10 for ideal nanostructures they are a consequence of long-range interface-induced correlations which can with good accuracy be related to the image charge potential. In recent years several equilibrium GW calculations have been reported (see for instance Refs. 11–16) showing in particular a renormalization of impurity or molecular levels near surfaces which again have the same origin. It was then quite natural to extend the GW method to out of equilibrium systems and to calculate the current within the Keldysh Green's function approach. This was done recently for simple systems in Refs. 17–19 laying a basis for a more accurate description of the conduction in such systems. The problem is that first principle GW calculations for realistic nanoscale devices are currently not feasible due to the huge computing cost.

We show in this paper that these effects can effectively be included in such devices on the basis of a simplified GW procedure. The poles of the exchange-correlation self-energy in the GW approximation occur at different plasmon frequencies. One can separate the contributions of different groups of plasmons. For some of them like interface plasmons, the corresponding contribution varies slowly in space and for large enough plasmon frequencies, the self-energy correction can be obtained accurately from the static limit of screening. By static we mean that the electron motion is slow enough that the screening cloud builds instantaneously around the electron position. In idealized situations the calculation then simply reduces to a conventional electrostatic image charge potential problem.

The paper is organized as follows. In a first part we discuss the origin of the interface-induced correlation effects and the methods to cope with them. Using the GW approximation we express the exchange-correlation self-energy in terms of the frequency dependent inverse dielectric matrix and discuss the corresponding plasmon poles. We identify the interface-induced correlation component by calculating the GW contribution arising from specific interface plasmon modes. Finally, as an application, we perform a calculation of this correlation effect on transport properties in a typical silicon nanowire metal-oxide-semiconductor field effect transistor (MOSFET) and discuss its influences as a function of size and dielectric mismatch.

II. THEORY

A. Interface-induced correlation effects

In open systems, the Hartree mean-field approximation does not include correlation effects corresponding to the fact that the moving electron repels the other electrons in its immediate vicinity. The electron must then be considered as a quasiparticle surrounded by a coulomb hole. This phenomenon corresponds to dynamic screening where the instantaneous total electron density n_{tot} exhibits a dip at the electron position $\mathbf{r}$. When this electronic reorganization is fast enough one can treat the screening of the charge as if it was static around the electron position. Let us discuss the features of this simple description in different situations: (i) for a bulk metal, the screening is complete. The total screening charge is $-e$ and occurs over a few Thomas-Fermi wavelengths. Conservation of the total charge implies that the compensating charge e is repelled at infinity; (ii) for a bulk semiconductor, screening is not complete. Beyond a few Thomas-Fermi wavelengths from the electron, the potential behaves as $e/\varepsilon|\mathbf{r}-\mathbf{r}'|$. Short-range screening corresponds to a coulomb hole with charge $-e(1-1/\varepsilon)$, with the compensating charge $e(1-1/\varepsilon)$ being also repelled to infinity; (iii) for semiconductor with boundaries, short-range screening again corresponds to a coulomb hole with charge $-e(1-1/\varepsilon)$, but now the compensating charge $e(1-1/\varepsilon)$ is the so-called image charge repelled at the boundaries. The interaction of the additional carrier with its own image charges gives rise to a screened self-energy correction. This self-energy correction has been addressed as a semiclassical screened self-energy in ideal semiconductor nanocrystallites, thin film and nanowires and shown to give an accurate correction to the band gap[5,20–22] when compared to *ab initio* calculations.

To improve the treatment of correlation effects while still using a single particle scheme one can use the LDA approximation. However this has limitations since it does not predict the correct semiconductor band gap and does not incorporate some long range correlation effects.[23] The GW approximation has been shown to provide accurate values for the gap of semiconductors.[23,24] Therefore it is of interest to include correlation effects in nanoscale devices along the lines of this method.

B. GW approximation

This method is based on an expansion of the exchange-correlation self-energy in terms of the dynamically screened electron-electron interactions. It was derived with field-theoretic techniques, Green's functions and the use of functional derivatives.[7] The expression for the exchange-correlation self-energy is then expressed in a way which evidences the role played by plasmons in renormalizing the electron-electron interactions. It allows to write an individual equation for a quasiparticle injected into a N electron system in terms of the properties of this N electron system. The GW Schrödinger equation for the excess electron can be written as

$$Hu_k(\mathbf{r}) = (H_0 + V_H)u_k(\mathbf{r}) + \int \Sigma(\mathbf{r},\mathbf{r}',\epsilon)u_k(\mathbf{r}')d\mathbf{r}', \quad (1)$$

where u_k is the quasiparticle wave function of energy ϵ_k, V_H is the Hartree potential energy of the N electron system, and Σ is the exchange-correlation self-energy given by[10]

$$\Sigma(\mathbf{r},\mathbf{r}',\epsilon) = -\sum_l u_l(\mathbf{r})u_l^*(\mathbf{r}')\left\{ n_l v(\mathbf{r},\mathbf{r}') + \sum_s V_s(\mathbf{r})V_s(\mathbf{r}') \times\left(\frac{n_l}{\epsilon_l-\epsilon-\omega_s} - \frac{1-n_l}{\epsilon-\epsilon_l-\omega_s}\right)\right\}, \quad (2)$$

where n_l is the occupation number of state u_l in the neutral system, v is the bare electron-electron interaction, and V_s is the potential induced by the fluctuation of electron density corresponding to a plasmon of frequency ω_s. It can also be shown[10] that the potential induced at position $\mathbf{r}'$ by a unit charge at $\mathbf{r}$ oscillating at frequency ω is

$$V_{ind}(\mathbf{r},\mathbf{r}',\omega) = \sum_s \frac{2\omega_s}{\omega^2-\omega_s^2}V_s(\mathbf{r})V_s(\mathbf{r}'). \quad (3)$$

For the following it will be more convenient to write this in matrix notation

$$V_{ind}(\omega) = \sum_s \frac{2\omega_s}{\omega^2-\omega_s^2}V_sV_s = [\varepsilon^{-1}(\omega)-I]v, \quad (4)$$

where $\varepsilon^{-1}(\omega)$ is the frequency dependent inverse dielectric matrix.

C. Discussion of $\varepsilon^{-1}(\omega)$ and plasmon poles

From Eqs. (2) and (4), the self-energy correction is related to the frequency dependent inverse dielectric matrix. In the following we examine how $\varepsilon^{-1}(\omega)$ can be calculated and how this can be applied to uniformly doped semiconductors. We anticipate the fact that screening due to valence electrons and to the small density gas of conduction electrons occurs in quite different frequency regimes. We then rewrite

$$\varepsilon(\omega) = [I - v\chi_v(\omega) - v\chi_c(\omega)] = [I - v\chi_v(\omega)]\{I - [I - v\chi_v(\omega)]^{-1}v\chi_c(\omega)\}, \quad (5)$$

where v is bare e-e interaction, χ_v and χ_c are polarizability matrices of valence and conduction electrons, respectively. In simplified form we can write the inverse dielectric matrix

$$\varepsilon^{-1}(\omega) = \varepsilon_c^{-1}(\omega)\varepsilon_v^{-1}(\omega), \quad (6)$$

where $\varepsilon_c^{-1}(\omega)=[I-\varepsilon_v^{-1}(\omega)v\chi_c(\omega)]^{-1}$ and $\varepsilon_v^{-1}(\omega)=[I-v\chi_v(\omega)]^{-1}$ are the inverse dielectric matrices of the conduction and valence electron system, respectively. Here we make use of Eq. (6) to discuss plasmons which are the poles of $\varepsilon^{-1}(\omega)$. Let us then analyze the frequency dependence of the inverse dielectric matrix in an average plasmon pole approximation in two cases: first for a dielectric, then for the n-doped semiconductor.

1. Dielectric (intrinsic silicon)

With no conduction electrons the bulk plasmon energies are the poles of the inverse dielectric matrix $\varepsilon_v^{-1}(\omega)$ corresponding to the valence electron system. The long wavelength pole has been shown to be given by[25]

$$(\hbar\omega_{sv})^2 = \frac{4\pi n_v e^2}{m}, \tag{7}$$

where n_v is the density of valence electrons. This turns out to give $\hbar\omega_{sv} \approx 16$ eV for bulk silicon. Taking this as the average plasmon energy Eq. (4) becomes

$$V_{ind}(\omega) = \frac{V_{ind}(\omega=0)}{1-\omega^2/\omega_{sv}^2} = \frac{(\varepsilon_v^{-1}(0)-1)v}{1-\omega^2/\omega_{sv}^2} \tag{8}$$

2. Doped bulk semiconductor

Here the system is composed of a filled valence band plus a small fraction of occupied states at the bottom of the conduction band. From Eq. (6) there are two types of poles. (1) Those of $\varepsilon_v^{-1}(\omega)$. As for intrinsic silicon, they correspond to the plasmon frequencies $\hbar\omega_{sv} \approx 16$ eV. (2) Those of $\varepsilon_c^{-1}(\omega) = [I - \varepsilon_v^{-1}(\omega) v \chi_c(\omega)]^{-1}$. The conduction electrons behave as a free-electron gas of low density, which, according to Eq. (7), should have a lower plasmon frequency for the long wavelength plasmons of the conduction electron gas. At these low frequencies $\varepsilon_v^{-1}(\omega) \approx \varepsilon_v^{-1}(\omega=0)$. Furthermore the matrix $\varepsilon_v^{-1}(0,r,r')$ simply reduces to $\frac{1}{\varepsilon}\delta(r-r')$ in $\varepsilon_c^{-1}(\omega)$, where ε is the long-range static dielectric constant of the intrinsic semiconductor. We can thus rewrite in the frequency range of interest

$$\varepsilon_c^{-1}(\omega) = \left[I - \frac{v}{\varepsilon}\chi_c(\omega) \right]^{-1}. \tag{9}$$

The corresponding plasmon energies of the conduction electrons are thus given by

$$(\hbar\omega_{sc})^2 = \frac{4\pi n_c e^2}{\varepsilon m^*}, \tag{10}$$

with $\varepsilon \simeq 11.7$ for silicon and $m^* \simeq 0.5$, we get $\hbar\omega_{sc} \approx 0.05$ eV, quite small compared to $\hbar\omega_{sv} \approx 16$ eV.

We can conclude that there are two regimes for doped semiconductors: low frequency corresponding to the conduction electrons with electron-electron interactions reduced by the bulk dielectric constant of the semiconductor; high frequency with $\varepsilon_c^{-1}(\omega)=1$ corresponding to the intrinsic semiconductor.

D. GW correction for confined systems

For a confined system, the determination of the self-energy given by Eq. (2) also requires a calculation of the plasmons which are the poles of the inverse dielectric matrices defined in Eqs. (5) and (6). However these dielectric matrices become different from their bulk counterpart since we have to include the influence of the interfaces. For reasons discussed before we separate the two regimes: (i) high frequencies corresponding to the intrinsic semiconductor and (ii) low frequencies corresponding to the gas of conduction electrons.

The existence of interfaces presents boundary conditions for the plasmons which are collective charge oscillations of the system. As shown in Ref. 25, in addition to the bulk plasmons, one can get solutions, which in the long wavelength limit are strictly localized at the interfaces. These are the interface plasmons. For silicon, the bulk plasmon is at about $\hbar\omega_{sb} \approx 16$ eV and the Si-SiO_2 interface plasmon at about $\hbar\omega_{sI} \approx 10$ eV.[25] In the expression of self-energy in Eq. (2), we can thus separate the contributions of bulk and interface plasmons. Bulk plasmons give a contribution contained in the bulk Hamiltonian of the semiconductor, while interface plasmons give an additional correction $\delta\Sigma_I$ written as

$$\delta\Sigma_I(\epsilon) = -\sum_{l,sI} V_{sI}(\mathbf{r}) V_{sI}(\mathbf{r}') u_l(\mathbf{r}) u_l^*(\mathbf{r}') \left\{ \frac{n_l}{\epsilon_l - \epsilon - \omega_{sI}} - \frac{1-n_l}{\epsilon - \epsilon_l - \omega_{sI}} \right\}, \tag{11}$$

corresponding to the contribution of interface plasmons in Eq. (2). Here V_{sI} is related to the potential induced by the fluctuation of charge density for the interface plasmon of frequency ω_{sI}. The same separation between bulk and interface plasmons can be made in Eq. (3), allowing to split V_{ind} into a bulk part and an interface contribution which we call V_I. From Eq. (3), $V_I(\mathbf{r},\mathbf{r}',\omega)$ is given by

$$V_I(\mathbf{r},\mathbf{r}',\omega) = \sum_{sI} \frac{2\omega_{sI}}{\omega^2 - \omega_{sI}^2} V_{sI}(\mathbf{r}) V_{sI}(\mathbf{r}'), \tag{12}$$

where the sum is restricted to interface plasmons. From Eq. (12), we calculate the interface contribution for a low-lying conduction band state u_c with energy ϵ_c

$$\delta\Sigma_I(\epsilon_c,\mathbf{r},\mathbf{r}') = -\sum_{l,sI} u_l(\mathbf{r}) V_{sI}(\mathbf{r}) V_{sI}(\mathbf{r}') u_l^*(\mathbf{r}') \left\{ \frac{n_l}{\epsilon_l - \epsilon_c - \omega_{sI}} - \frac{1-n_l}{\epsilon_c - \epsilon_l - \omega_{sI}} \right\}. \tag{13}$$

We now anticipate the fact that V_{sI} is slowing varying in space over the active region and will discuss the validity of this approximation later. V_{sI} will then mix u_c with states which have similar wave function and energy. The sum in the above equation can then be restricted to empty states $u_l \simeq u_c$, the energies $\epsilon_c - \epsilon_l$ being negligible with respect to ω_{sI}. Thus only the second part in the sum survives and we can neglect $\epsilon_c - \epsilon_l$ compared to ω_{sI}. We then obtain

$$\delta\Sigma_I(\mathbf{r},\mathbf{r}') = -\sum_{l,sI} u_l(\mathbf{r}) \frac{V_{sI}(\mathbf{r}) V_{sI}(\mathbf{r}')}{\omega_{sI}} u_l^*(\mathbf{r}'). \tag{14}$$

Using Eq. (12) in the limit $\omega \to 0$, we can rewrite this as[23]

$$\delta\Sigma_I(\mathbf{r},\mathbf{r}') = \frac{1}{2}\sum_l u_l(\mathbf{r}) V_I(\mathbf{r},\mathbf{r}',\omega=0) u_l^*(\mathbf{r}'). \tag{15}$$

This equation can be simplified by noticing that $\Sigma_l u_l(\mathbf{r}) u_l^*(\mathbf{r}')$ is invariant upon any unitary transformation of conduction states. In particular we can define for the bulk Wannier functions, which have a localized character. We thus have $\Sigma_l u_l(\mathbf{r}) u_l^*(\mathbf{r}') = \Sigma_j W_j(\mathbf{r}) W_j^*(\mathbf{r}')$, where j is a bond index. For a slowly varying potential, $(V_I)_{jj'} = (V_I)_{jj}\delta_{jj'}$, which leads to

$$\delta\Sigma_I(\mathbf{r},\mathbf{r}') = \frac{1}{2}\sum_j W_j(\mathbf{r})W_j^*(\mathbf{r}')(V_I)_{jj}, \tag{16}$$

where $(V_I)_{jj}$ is the value at site j. In the same basis this is equivalent to write that the self-energy reduces to a local function

$$\Sigma(\mathbf{r}) = \Sigma_I(\mathbf{r},\mathbf{r}) = \frac{1}{2}V_I(\mathbf{r},\mathbf{r},\omega=0), \tag{17}$$

where $\Sigma(\mathbf{r})$ reduces to the interface-induced static image self-energy.

This approximation is similar to the one developed in Ref. 7 as COHSEX (Coulomb hole plus statically screened exchange). The main difference is that here it is used for conduction states and interface contributions while COHSEX was applied to the whole band structure and the full self-energy which is less justified. Let us now comment on the fact that we have considered the V_{sI} to be slowly varying over the active device region. This might seem unreasonable since it is known that classical image potentials diverge at the interface. The simplest example is the metal-dielectric interface where the self-energy would behave as $-e^2/(\varepsilon.d)$, ε being the dielectric constant, and d the distance of the charge e to the interface. However, this divergence is related to the fact that, in the classical limit, the interface charge is strictly localized on the interface plane. It would not subsist in microscopic calculations where the charge oscillations corresponding to plasmons should extend over the screening length characteristic of the material. This was proven by Newns[26] for the metal-dielectric interface who obtained a self-energy $-e^2/[\varepsilon.(d+2\lambda)]$ for $d\to 0$ where λ is the Thomas-Fermi screening length, of the order of the interatomic spacing or more. The true potential will then saturate at a distance of the order 2λ leading to a much smoother spatial variation. Another point is that the transverse wave function is vanishingly small in the silicon-oxide interface region reducing the corresponding contribution. All these arguments are confirmed by the results of Ref. 21 for ideal nanostructures showing that the assumption of slowly varying V_{sI} gives practically exact results even for extremely small nanostructures (down to 1 nm).

III. APPLICATION TO NANOWIRE MOSFETS

As an application of the GW calculation of the interface-induced correlation effect in realistic nanostructures, we consider in this section the gate-all-around silicon nanowire transistor shown in Fig. 1.

The determination of the interface-induced potential requires the calculation of the effect of the image charges on the dielectric interfaces. We then solve the Poisson equation for a test charge located at $\mathbf{r}$ producing a potential $V(\mathbf{r},\mathbf{r}')$ at position $\mathbf{r}'$ satisfying $\nabla_{r'}[\varepsilon(\mathbf{r}',\omega)\nabla_{r'}V(\mathbf{r},\mathbf{r}')] = -4\pi e\delta(\mathbf{r}-\mathbf{r}')$. The resulting solution can be written as $V(\mathbf{r},\mathbf{r}') = V_I(\mathbf{r},\mathbf{r}') + V_b(\mathbf{r},\mathbf{r}')$ where $V_b(\mathbf{r},\mathbf{r}') = \frac{e}{\varepsilon|\mathbf{r}-\mathbf{r}'|}$ is the potential in the bulk semiconductor and $V_I(\mathbf{r},\mathbf{r}')$ is the potential created by the image charges on the dielectric interfaces. At this stage we use the dynamical dielectric constant ($\varepsilon_{ox}^{\infty}=2.1$ for SiO2) containing only the electronic contribution,[27] since the dynamics of the ions in the oxide is much slower than those of the electrons. $\varepsilon_{ox}^{\infty}$ is evaluated at a frequency above the highest optical phonon modes of the oxide. Once $V_I(\mathbf{r},\mathbf{r}')$ is obtained, we can calculate the GW self-energy correction accordingly.

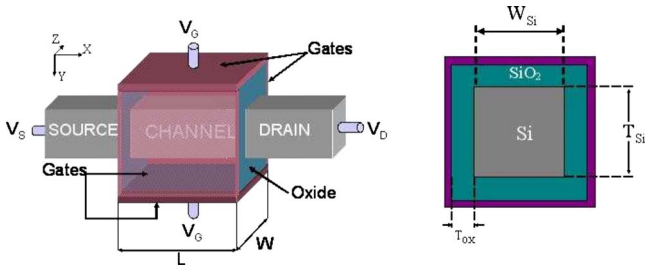

FIG. 1. (Color online) Structure of the silicon nanowire MOSFET ⟨100⟩ oriented considered in this work. The length of source, drain, and channel is 8 nm each. The oxide thickness is set as 1 nm. Continuous doping of 2×10^{20} cm^{-3} is assumed in source and drain whereas the channel is intrinsic.

One point concerns the conduction electron influence. We have already argued in Sec. II C that at the high frequencies characteristic of the SiO2 interface plasmons, their contribution to the dynamical inverse dielectric matrix is negligible. Furthermore their concentration in the channel is very low and we numerically checked that they do not have any significant influence on the image charge potential in the range of sizes of interest.

The transport formalism is based on the Landauer-Büttiker formula.[28] The three-dimensional (3D) Schrödinger equation is expressed within the effective mass approximation whose values have been renormalized for each cross-section from tight-binding band structure calculations.[29] This approach has demonstrated to correctly describe ⟨100⟩-oriented silicon nanowires with diameter down to 2 nm.[30] We then add the self-energy correction to the usual electrostatic potential and solve self-consistently the Poisson and Schrödinger equations. The transport properties are com-

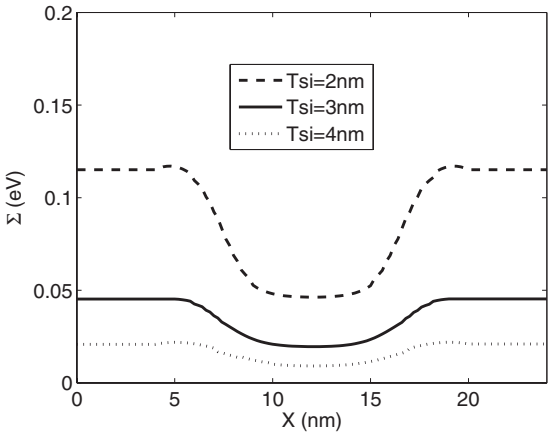

FIG. 2. The interface-induced self-energy correction Σ along the transport direction taken in the middle of the cross-section for transistors with different silicon thickness T_{Si}. The surrounding metal gate extends from 8 to 16 nm.

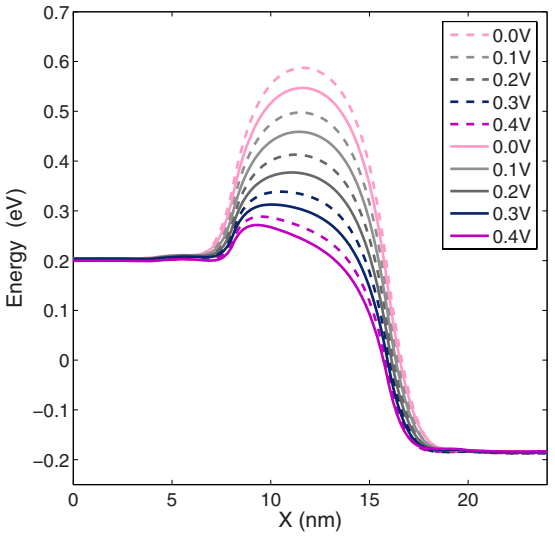

FIG. 3. (Color online) Electron subband profile at different gate voltages (from 0.0 to 0.4V) with Σ (solid line) and without Σ (dash line). Here T_{Si}=3 nm; V_{DS}=0.4 V.

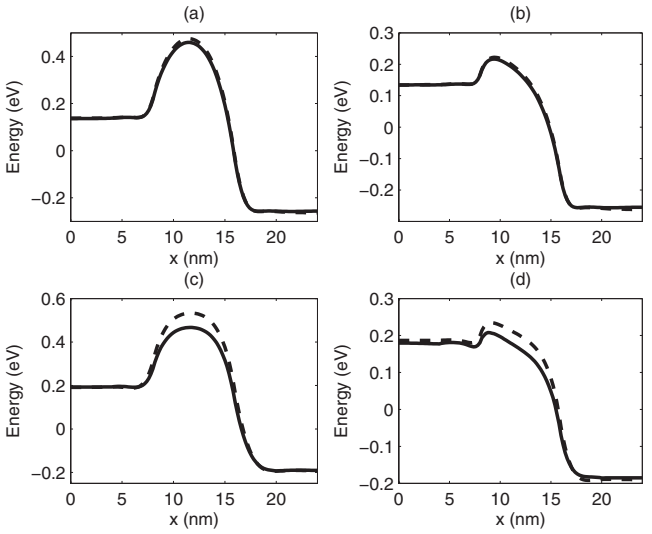

FIG. 4. Electron subband profile for transistors with Σ (solid line) and without Σ (dash line) at different parameters: (a) T_{Si} =4 nm, V_G=0.0 V; (b) T_{Si}=4 nm, V_G=0.4 V; (c) T_{Si}=2 nm, V_G=0.0 V; and (d) T_{Si}=2 nm, V_G=0.4 V.

puted within the mode-space Green's function formalism which consists in separating the 3D Schrödinger equation into a two-dimensional equation describing the confinement in the cross-section and a one-dimensional equation defining the ballistic transport along the nanowire axis. The system is then defined by independent electron subbands (numbered by the index i) for which the retarded Green's function is expressed as follows:

$$G_i(E) = [E - H_i - \Sigma_D^i - \Sigma_S^i]^{-1}, \tag{18}$$

where E is the energy, H_i is the ith subband Hamiltonian including the electrostatic potential and the self-energy correction Σ, whereas Σ_D^i and Σ_S^i are the self-energies induced by the coupling with the source and drain reservoirs.[10] From Eq. (18), one can calculate the electron densities and the drain current resulting from the lowest subbands of each valley. This approach has been evidenced to give accurate results for macroscopic potential variations.[31–35]

The self-energy correction Σ along the transport direction at the middle of the cross-section is shown in Fig. 2 for various diameters. We first note that the additional potential presents smooth spatial variations and we have checked that it does not induce significant coupling between electron subbands. Moreover, it is continuously positive inside the silicon nanowire since $\varepsilon_{si} > \varepsilon_{ox}^{\infty}$, which is consistent with previous theoretical predictions.[5,10] The influence of the gate, which extends from 8 to 16 nm, is also clearly visible. It induces a larger screening and therefore reduces the self-energy in the channel compared with its value in the source and drain regions. At T_{Si}=4 nm, the interface influence is quite small and Σ tends to be constantly small all along the source-drain axis. The electrons do not experience any particular perturbation. When reducing the silicon thickness from 4 to 2 nm, the dynamical screening of the gate starts to have a significant impact on the electrons in the channel and the difference in amplitude between the self-energy in the channel and in the lateral regions increases rapidly to reach 0.07 eV at 2 nm. Figure 3 shows the first electron subband with and without the self-energy corrections at different gate voltages with T_{Si}=3 nm. We observe a systematic reduction in the barrier potential in the channel whatever the applied gate voltage. In order to better illustrate the cross-section dependence Fig. 4 shows the modifications of the first electron subband in devices with T_{Si}=4 nm and 2 nm at two different gate voltages. We can note that Σ has a minor influence in a nanowire of 4 nm whereas the channel potential barrier undergoes a major decrease in almost 0.1 eV in devices with T_{Si}=2 nm independently of the applied gate voltage. This situation has a direct consequence for the current-voltage characteristics

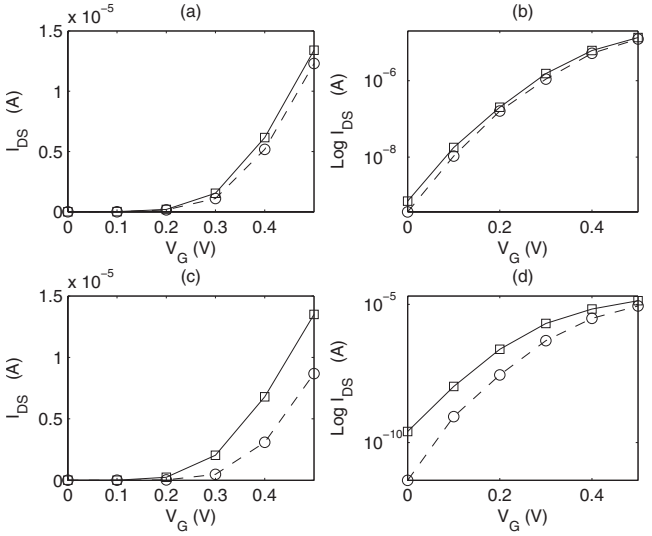

FIG. 5. Comparison of the I_D vs V_G characteristics at V_{DS} =0.4 V for different silicon nanowire transistors embedded by oxide SiO_2 with Σ (solid line) and without Σ (dashed line). (a) T_{Si} =4 nm, (b) T_{Si}=4 nm, (c) T_{Si}=2 nm, and (d) T_{Si}=2 nm.

shown in linear and logarithmic scale in Fig. 5. Although the modifications are quite weak for a 4 nm cross-section, the self-energy correction dramatically increases the current by one order of magnitude in nanowires of 2 nm. This effect has then a remarkable influence in ultimate nanowire MOSFETs and must be taken into account in the device quantum simulation tools.

IV. CONCLUSION

In conclusion, we have discussed the importance of interface-induced correlation effects in realistic nanoscale structures through an investigation of the corresponding GW exchange-correlation self-energy. We estimate the influence of these correlation effects on the transport properties of realistic nanoscale devices. For nanowire transistors with a diameter below 4 nm, the interface-induced self-energy correction can shift the electron subbands significantly in the channel region and therefore has a great influence on current-voltage characteristics. With the decrease in size, interface-induced correlation effects are increasingly important and could contribute to intensify the current variability in ultimate nanoscale transistors. This approach can be extended in a straightforward manner to other nanoscale devices with various geometries.

ACKNOWLEDGMENT

This work is supported by the QUANTAMONDE contract (ANR-07-NANO-023) funded by the ANR-French National Research Agency.

*marc.bescond@im2np.fr

[1] Y. Cui and C. M. Lieber, Science **291**, 851 (2001).
[2] X. Duan, C. Niu, V. Sahi, J. Chen, J. W. Parce, S. Empedocles, and J. L. Goldman, Nature (London) **425**, 274 (2003).
[3] X. Guo and S. R. P. Silva, Science **320**, 618 (2008).
[4] C. Cen, S. Thiel, J. Mannhart, and J. Levy, Science **323**, 1026 (2009).
[5] Y.-M. Niquet, A. Lherbier, N. H. Quang, M. V. Fernandez-Serra, X. Blase, and C. Delerue, Phys. Rev. B **73**, 165319 (2006).
[6] M. Diarra, Y.-M. Niquet, C. Delerue, and G. Allan, Phys. Rev. B **75**, 045301 (2007).
[7] L. Hedin and S. Lundqvist, Solid State Phys. **23**, 1 (1970).
[8] J. C. Inkson, J. Vac. Sci. Technol. **11**, 943 (1974).
[9] J. P. A. Charlesworth, R. W. Godby, and R. J. Needs, Phys. Rev. Lett. **70**, 1685 (1993).
[10] C. Delerue and M. Lannoo, *Nanostructures-Theory and Modelling* (Springer-Verlag, Berlin, 2004).
[11] P. Rinke, K. Delaney, P. Garcia-Gonzalez, and R. W. Godby, Phys. Rev. A **70**, 063201 (2004).
[12] S. Crampin, Phys. Rev. Lett. **95**, 046801 (2005).
[13] M. Rohlfing, N.-P. Wang, P. Krüger, and J. Pollmann, Phys. Rev. Lett. **91**, 256802 (2003).
[14] C. Freysoldt, P. Rinke, and M. Scheffler, Phys. Rev. Lett. **103**, 056803 (2009).
[15] J. B. Neaton, M. S. Hybertsen, and S. G. Louie, Phys. Rev. Lett. **97**, 216405 (2006).
[16] K. S. Thygesen and A. Rubio, Phys. Rev. Lett. **102**, 046802 (2009).
[17] K. S. Thygesen and A. Rubio, J. Chem. Phys. **126**, 091101 (2007).
[18] P. Darancet, A. Ferretti, D. Mayou, and V. Olevano, Phys. Rev. B **75**, 075102 (2007).
[19] C. D. Spataru, M. S. Hybertsen, S. G. Louie, and A. J. Millis, Phys. Rev. B **79**, 155110 (2009).
[20] C. Delerue, G. Allan, and M. Lannoo, Phys. Rev. Lett. **90**, 076803 (2003).
[21] C. Delerue, M. Lannoo, and G. Allan, Phys. Rev. Lett. **84**, 2457 (2000).
[22] C. Freysoldt, P. Eggert, P. Rinke, A. Schindlmayr, and M. Scheffler, Phys. Rev. B **77**, 235428 (2008).
[23] W. G. Aulbur, L. Jonsson, and J. W. Wilkins, Solid State Phys., Adv. Res. Appl. **54**, 1–218 (1999).
[24] R. O. Jones and O. Gunnarsson, Rev. Mod. Phys. **61**, 689 (1989).
[25] C. Kittel, *Introduction to Solid State Physics* (Wiley, New York, 1996).
[26] D. M. Newns, J. Chem. Phys. **50**, 4572 (1969).
[27] M. Diarra, C. Delerue, Y.-M. Niquet, and G. Allan, J. Appl. Phys. **103**, 073703 (2008).
[28] M. Büttiker, Y. Imry, R. Landauer, and S. Pinhas, Phys. Rev. B **31**, 6207 (1985).
[29] K. Nehari, N. Cavassilas, F. Michelini, M. Bescond, J. L. Autran, and M. Lannoo, Appl. Phys. Lett. **90**, 132112 (2007).
[30] J. Wang, A. Rahman, A. Ghosh, G. Klimeck, and M. Lundstrom, IEEE Trans. Electron Devices **52**, 1589 (2005).
[31] J. Wang, E. Polizzi, and M. Lundstrom, J. Appl. Phys. **96**, 2192 (2004).
[32] M. Bescond, K. Nehari, J. L. Autran, N. Cavassilas, D. Munteanu, and M. Lannoo, Tech. Dig. - Int. Electron Devices Meet. **2004**, 617.
[33] S. Jin, M. V. Fischetti, and T.-W. Tang, J. Appl. Phys. **102**, 083715 (2007).
[34] K. Nehari, N. Cavassilas, J. L. Autran, M. Bescond, D. Munteanu, and M. Lannoo, Solid-State Electron. **50**, 716 (2006).
[35] M. Luisier, A. Schenk, and W. Fichtner, J. Appl. Phys. **100**, 043713 (2006).